Environmental Science
Processes & Impacts

Accepted Manuscript

This article can be cited before page numbers have been issued, to do this please use: K. Bright, B. Dienes, B. van Dongen, I. Strashnov, X. Han and M. Aeppli, *Environ. Sci.: Processes Impacts*, 2026, DOI: 10.1039/D5EM01047K.

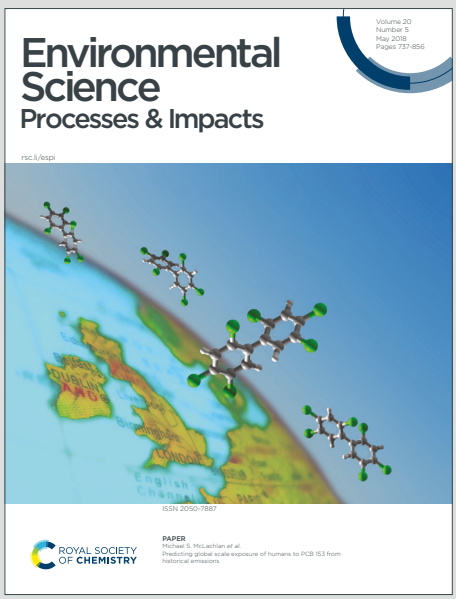

ROYAL SOCIETY OF CHEMISTRY

rsc.li/espi

View Article Online
DOI: 10.1039/D5EM01047K

Emerging investigator series: Metagenomic Insights Into Microbial Controls of Carbon Cycling in Alpine Soils

Kristina Bright[1], Bence Dienes[1], Bart van Dongen[2], Ilya Strashnov[2], Xingguo Han[3], Meret Aeppli[1*]

[1]Soil Biogeochemistry laboratory (SOIL), Swiss Federal Institute of Technology Lausanne (EPFL), Sion, Switzerland

[2]Department of Earth and Environmental Sciences, University of Manchester, Manchester, United Kingdom

[3]Swiss Federal Institute for Forest, Snow and Landscape Research (WSL), Birmensdorf, Switzerland

[*] correspondence: meret.aeppli@epfl.ch, +41 21 693 72 79

Abstract: Alpine riparian zones span topographic gradients from wet soils on the plain near streams to drier soils on adjacent slopes. These differences in soil moisture are generally associated with shifts in soil redox state from anoxic on the plain to oxic on the slope. In anoxic plain soils, soil organic carbon (SOC) may accumulate due to thermodynamic constraints on microbial activity. Here, we used shotgun metagenomics to examine how microbial diversity and functional potential varies across differing redox conditions on plain and slope soils in two catchments in the Swiss Alps. We complemented these analyses with soil physicochemical characteristics and information on the chemical composition of organic matter. Plain soils had higher SOC stocks and higher relative abundance of phenol compounds relative to slope soils, consistent with SOC preservation and preferential mineralisation of easily degradable organic compounds under anoxic conditions. Microbial communities in plain soils further exhibited greater taxonomic and functional diversity, including an increased potential for anaerobic respiration pathways. Genes for nitrate, iron, and sulfate reduction were linked to *Chloroflexota*, *Acidobacteria*, and *Desulfobacterota* phyla, respectively. Based on NMDS correlations, electron accepting capacity, calcium content, and pH shaped microbial community composition. Slope soils, by contrast, supported less diverse microbial communities, determined mainly by electron donating capacity and clay content. Our work demonstrates how soil redox conditions and microbial functional potential shape carbon cycling across landscape positions in alpine riparean zones. This mechanistic understanding is critical to anticipate changes in carbon cycling in alpine ecosystems in a changing climate.

Keywords: Soil organic carbon, soil redox dynamics, microbial community composition, microbial metabolism, Alpine riparian soils, shotgun metagenomics

Introduction

In subalpine and alpine ecosystems, more than 90% of ecosystem carbon are stored in soils as a consequence of short plant growing seasons and limitations on the degradation of soil organic matter by microorganisms under harsh climatic conditions [1,2]. The fate of organic

View Article Online
DOI: 10.1039/D5EM01047K

carbon in the soil is determined by microorganisms that can mineralize organic matter to greenhouse gases or stabilize it within soils [3,4]. It remains unclear how SOC stocks are linked to microbial community composition and functional potential in (sub)alpine ecosystems.

Alpine riparian zones express strong differences in hydrology and soil biogeochemistry between soils on low-lying plains near streams to those on adjacent slopes [5,6]. Plain soils, influenced by shallow groundwater and seasonal water inputs, are periodically saturated, producing oxygen-limited redox conditions where microbial respiration depends on alternative terminal electron acceptors (TEAs). These less energy-efficient pathways slow organic matter decomposition and promote SOC accumulation [7–10]. In contrast, slope soils are well drained and maintain more oxidized conditions that support aerobic microbial activity and greater SOC mineralization, resulting in smaller SOC stocks relative to plains [11].

Soil redox conditions, along with other edaphic factors such as pH and nutrient availability, are linked to microbial community composition and metabolic diversity [12]. Microbial characteristics can be assessed using metagenomics, which has proven particularly valuable in extreme environments such as thawing permafrost, where genomic analyses have revealed microbial adaptations to redox-stratified conditions and geochemical gradients [13–15]. [13], for instance, showed that imicrobial iron reduction strongly influences microbial carbon degradation in thawing permafrost. Similarly, [14] demonstrated that permafrost microbial communities and functional genes are structured by latitudinal gradients and soil geochemistry. In alpine plains, fluctuating water tables and variable oxygen conditions likely necessitate a wide microbial metabolic repertoire, enabling microorganisms to adapt their respiration strategies to the availability of TEAs [10,16,17]. Alpine systems therefore express similar redox variability and potentially microbial adaptation strategies as thawing permafrost, yet integrated metagenomic assessments remain rare in alpine environments.

Here, we investigate the relationships between SOC stocks, microbial community structure and functional potential, and environmental conditions across plain and slope areas in two alpine headwater catchments. Although environmental conditions differ slightly between the two catchments, both share similar geomorphic structures and hydrological regimes and can therefore be treated as landscape-level replicates. We hypothesise that:

1. Plain soils exhibit anoxic conditions that are associated with higher SOC contents and higher levels of poorly degradable SOC, such as phenols and aromatics.

2. Microbial communities exhibit greater metabolic diversity in plain than slope soils due to larger temporal variability in soil redox conditions.

To test our hypotheses, we combine the analysis of soil physicochemical characteristics with analyses of soil redox state by mediated electrochemistry, soil organic matter chemistry by pyrolysis gas chromatography-mass spectrometry, and microbial functional diversity and metabolic capabilities by shotgun metagenomics. We compared SOC content and composition across landscape positions and soil depths, correlated taxonomic lineages with functional gene potentials, and incorporated environmental vectors into a non-metric

View Article Online
DOI: 10.1039/D5EM01047K

multidimensional scaling (NMDS) ordination analysis to assess the relationships between microbial communities and environmental factors.

Materials and Methods

Site Description and Sample Collection

Soils were collected from the riparean areas of two natural headwater catchments in the Swiss Alps: Blatt in the Binntal valley (46°22'N/8°16'E) and Ar du Tsan (46°12'N/7°30'E) in the Vallon de Réchy. Both catchments feature a mixed bedrock mainly comprised of gneiss and carbonated rock (Matteodo et al., 2018; swisstopo, 2024). They are characterised by siliceous alpine grasslands and moorlands. Vegetation differs systematically between slope and plain positions. Slope areas are dominated by subalpine acidophilous grassland and heath communities, whereas plain areas support wetland vegetation typical of alkaline and acidophilic fens. Reported plant community types include *Nardion*, *Rhododendro-Vaccinion*, and *Loiseleurio-Vaccinion* on slopes, and *Caricion davallianae*, *Caricion fuscae*, *Calthion*, and *Caricetum rostratae* on plains [18–20]. The sampling sites within the two catchments were strategically chosen to encompass both slope and plain areas. At Réchy, the elevation of sampling locations varied from 2154 to 2243 meters above sea level (m a.s.l.), while at Binntal, the range was between 1984 and 2105 m a.s.l. Soil sampling was carried out in late July 2023. Average July temperatures at l'Ar du Tsan and Binntal are 12.9 °C and 8.7 °C, with precipitation levels of 76 mm and 97 mm, respectively [21]. At 8 sampling locations (Figure 1 and Table S1), soil from three soil depths (0-10 cm, 10-30 cm, and 30-50 cm, when available) was collected with an auger. Precise coordinates, slope, and specific landscape position were recorded for each location. Once gathered, the samples were placed in zip-lock bags; bags for water-logged soils contained oxygen scrubbers. Samples were kept cool with ice packs, and transported to the laboratory. Samples for soil physicochemical characterization were immediately processed; sub-samples for soil redox characterization were stored at -20 °C until analysis. Samples for DNA extraction were placed in a sterile manner into Whirl-Pack® bags and homogenised directly by kneading. Post-homogenisation, the soil was split into triplicate subsamples, put into cryotubes snd shock-frozen using liquid nitrogen. After transport to the laboratory, they were stored at -80 °C until analysis.

View Article Online
DOI: 10.1039/D5EM01047K

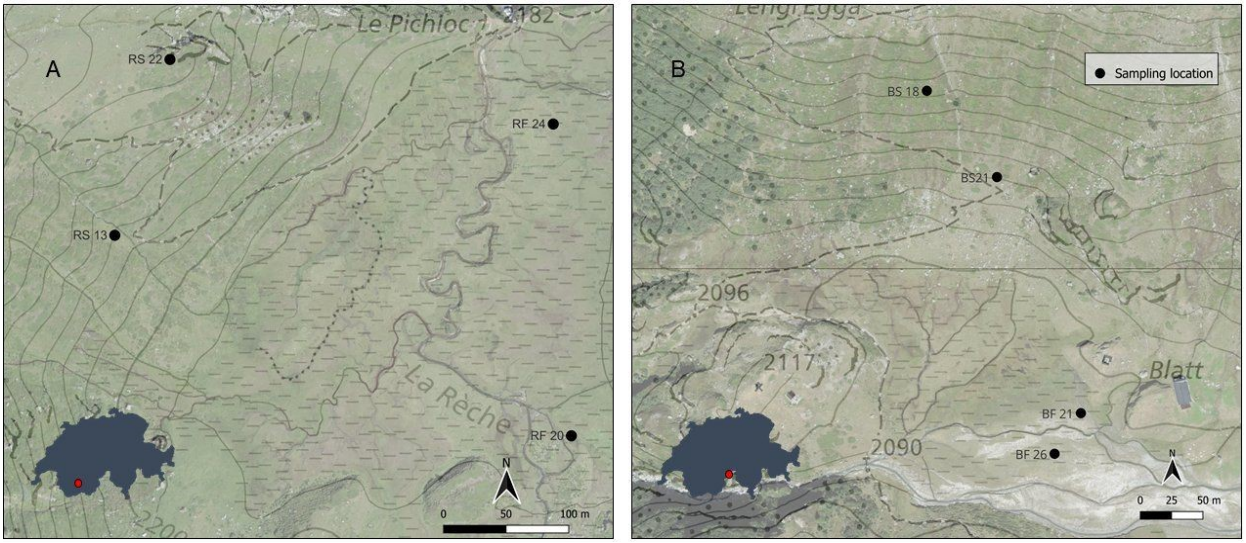

Figure 1: Sampling locations in Réchy and Binntal showing the spatial layout of plain and slope sites across the two catchments. The map is intended to provide site context; depth-specific SOC differences are presented separately in Figure 2. Locations where the 30–50 cm interval was unavailable are indicated in Table S1.

Soil Physicochemical Characterisation

Sample preparation, pH measurements, and soil texture analyses: Soil samples were air-dried and subsequently oven-dried at 105°C, homogenised, sieved through a 2 mm mesh to remove coarse particles (e.g., plant roots and stones), and ground using a ball mill (Pulverisette 7, Fritsch) to achieve a fine, uniform powder. Dry weight was determined from changes in soil mass upon drying. Soil pH was measured SevenDirect SD50 pH meter, Mettler Toledo) in a 1:5 soil-to-deionised water suspension after 30 minutes of agitation at 200 RPM, followed by 30 minutes of settling (Table S1). Soil texture was analysed using laser diffraction (LS 13 320, Beckman Coulter) with a grain size analyser, on 0.5 g of air-dried, sieved bulk soil following organic matter digestion with hydrogen peroxide over two weeks (Table S1).

Elemental composition: Total carbon was measured by chromatography after combustion at 900 °C on a CHNS element analyser (Flash EA 1112, Thermo Finnigan). As the soils lacked carbonates, the total SOC content (expressed as weight % of dry soil) was considered equivalent to the measured total carbon. Total content of Fe, Mn, and S were determined on 5 g of dried, sieved, and powdered soil using X-ray fluorescence spectroscopy (SPECTRO XEPOS).

SOC composition: The relative abundance of major compound classes were determined using pyrolysis gas chromatography–mass spectrometry (Py-GC-MS, [22]. Soil samples were placed in clean, fire-polished quartz tubes and pyrolysed at 600°C for 20 seconds under a helium flow. The released pyrolysis moieties were transferred via a heated transfer line into an Agilent 7980A GC equipped with a Zebron ZB-5MS column (Phenomenex, Woerden, the Netherlands; 30 m × 250 μm × 0.25 μm) coupled to an Agilent 5975C MSD single quadrupole mass spectrometer operating in electron ionisation mode (scanning *m/z* 50 to 650 at 2.7

View Article Online
DOI: 10.1039/D5EM01047K

scans per second; ionisation energy: 70 eV), using helium as the carrier gas and introduced in split mode (70: 1 split ratio; constant flow of 2 ml per min, with gas saver mode active). The pyrolysis transfer line and rotor oven temperature were maintained at 325°C, the heated GC interface at 280°C, the electron ionisation source at 230°C, and the quadrupole at 150°C. The GC oven was programmed from 40°C (held for 5 minutes) to 300°C at 5°C per minute, where it was held for 3 minutes, giving a total run time of 60 minutes. Approximately 106 of the most abundant pyrolysis moieties were identified, identified by comparing their retention times and spectra to entries in the NIST Mass Spectral Library and grouped into categories based on their origin and chemical characteristics: lipids, lignins, polysaccharides, phenols, nitrogen containing compounds, and aromatics (Figure S1). Given the complexity of the pyrograms, it was not possible to integrate individual moiety in total ion current mode due to significant overlap between ion peaks. Instead, single ion filtering was used to measure the peak area of each compound. The major ions of each compound were filtered and integrated (Table S2). The relative abundance of each identified compound was calculated as a percentage of the total identified compounds.

Electron accepting & donating capacities: Electron accepting and electron donating capacities (EAC & EDC), were determined through mediated electrochemical analyses using an 8-channel potentiostat (CH Instruments, Inc.) in an anoxic environment inside a glovebox workstation (Labmaster pro MBraun), as previously described [23,24]. Experiments were conducted using a pH-buffered solution at pH 5.5 (0.4 M sodium acetate-acetic acid) with 10 mM sodium chloride as a background electrolyte. Mediated electrochemical reduction (MER) potentials were set versus standard hydrogen electrodes at -0.51 V vs. SHE ($E_{\mathrm{H,\,MER}}$) and mediated electrochemical oxidation (MEO) potentials at +0.82 V vs. SHE ($E_{\mathrm{H,\,MEO}}$). For EAC measurements, ethyl viologen [25] was used as an electron transfer mediator; for EDC, ABTS [26] was used. To prepare the samples, 1 of frozen soil was transferred into 10 of Milli-Q water under anaerobic conditions to create a slurry. For each measurement, 30 of the slurry was used for EAC determination, and 20 for EDC determination. An additional 1 aliquot was taken from each slurry in triplicate to determine soil dry weight for normalisation. During EAC determination, electrons are delivered from the electrode via the mediator to the sample's redox reactive constituents, thereby reducing them. Conversely, during EDC measurement, electrons are withdrawn from these constituents through the mediator and transferred to the electrode. EAC and EDC values were determined from current responses measured upon the addition of the sample to the electrochemical cells at $E_{\mathrm{H,\,MER}}$ and $E_{\mathrm{H,\,MEO}}$, respectively. Capacities (mol e^- g^{-1} dried soil) were determined by integrating the baseline-corrected current, $i(t)$, over time from t_0 until the current returned to baseline at t_{end} following equations 1 and 2.

$$\mathrm{EAC} = \frac{1}{F \times m_{\mathrm{sample}}} \int_{t_0}^{t_{\mathrm{end}}} i\,(t)\,\mathrm{d}t$$

$$\mathrm{EDC} = -\frac{1}{F \times m_{\mathrm{sample}}} \int_{t_0}^{t_{\mathrm{end}}} i\,(t)\,\mathrm{d}t$$

where $F \approx 96485\ \mathrm{C\,mol^{-1}}$ is the Faraday constant and m_{sample} is the dry mass of the soil.

View Article Online
DOI: 10.1039/D5EM01047K

DNA Extraction, Sequencing, and Analysis

DNA was extracted from 0.5 g of soil using the DNeasy PowerSoil Pro Kit (Qiagen, Germany) following the manufacturer's protocol. DNA integrity was assessed using an Agilent 5400 system. DNA content and purity were assessed using microspectrophotometry (NanoDrop One; Thermo Fisher Scientific Inc., USA). Library preparation and shotgun metagenomic sequencing were performed by Novogene (UK) with Illumina NovaSeq 6000 platform to generate paired-end (150 bp) reads. Across the 20 samples, sequencing yielded an average of 103.7 million raw reads per sample (range: 83.7–132.1 million), corresponding to an average of 15.5 Gb raw data per sample (range: 12.6–19.8 Gb). Assembly quality was evaluated using QUAST; across 19 assemblies, the average total contig length was 673.7 Mb (range: 422.7–1094.5 Mb) and the average N50 was 979 bp (range: 783–1395 bp).

Initial quality checks of raw sequencing reads were conducted using FastQC to ensure data integrity [27]. Reads were subjected to quality filtering using fastp [28], followed by a second round of quality checks with FastQC to verify improvements in read quality. De novo assembly of high-quality reads was performed with MEGAHIT, generating contigs suitable for downstream analyses [29]. Assembly statistics were evaluated using QUAST to ensure completeness and accuracy [30]. High-quality reads were mapped to assembled contigs using Strobealign to generate coverage profiles [31]. Metagenome-assembled genomes (MAGs) were reconstructed using MetaBAT2 [32], and bin quality was assessed using CheckM2 to ensure completeness and contamination metrics were within acceptable thresholds [33]. Taxonomic classification of MAGs was assigned using the Genome Taxonomy Database Toolkit (GTDB-Tk, [34]. Functional annotation of MAGs was conducted using METABOLIC [35], allowing for the prediction of key metabolic pathways and biogeochemical functions. Dereplication of MAGs was performed using dRep to consolidate redundant genomes and generate a representative set [36]. The relative abundance of dereplicated MAGs was calculated using CoverM [37].

Statistical Analysis

SOC content and composition were analysed using Wilcoxon rank-sum tests for comparison of plain and slope soils and one-way ANOVA with Tukey's HSD post-hoc tests for soil depth effects. Spearman correlations were used to examine associations between functional gene categories and taxonomic lineages identified in the metagenomic data. Non-metric multidimensional scaling (NMDS) analysis was used to to visualise microbial community dissimilarities based on Bray-Curtis distances and identify effects of environmental factors on microbial community composition. This analysis was complemented by a PERMANOVA test to assess the influence of location, landscape position, and soil depth on microbial community structures. Figures and statistical analyses were generated in R using the vegan package to explore microbial community composition and diversity metrics [38].

View Article Online
DOI: 10.1039/D5EM01047K

Results

Plain Soils Store More Organic Carbon Than Slope Soils

Plain soils had higher SOC contents than slope soils at all soil depths (Figure 2): SOC ranged was 24.3 ± 8.3% in the 0 - 10 cm layer and 22.8 ± 20.5% at 30 - 50 cm. with highest SOC values observed in the mid-soil depth layer (10 - 30 cm: 29.6 ± 16.3%) for plain soils. In contrast, slope soils exhibited a clear soil depth-dependent trend in SOC concentrations, with SOC decreasing from 6.49 ± 4.92% in the surface layer (0 - 10 cm) to 2.48 ± 0.66% at 10 - 30 cm, and 1.80 ± 0.20% at 30 - 50 cm. SOC content in plain soils was significantly higher than that of the slope across all soil depths, with mean SOC at 0 - 10 cm soil depth in plain soils being approximately 3.7 times higher than in slope soils. The spatial distribution of SOC stocks is shown in Figure 1. In both the Réchy and Binntal catchments, plain soils in unshaded terrain showed higher SOC (Réchy: 10 - 30%, Binntal: 20 - 42%), while shaded slope soils were lower (2 - 10% for both).

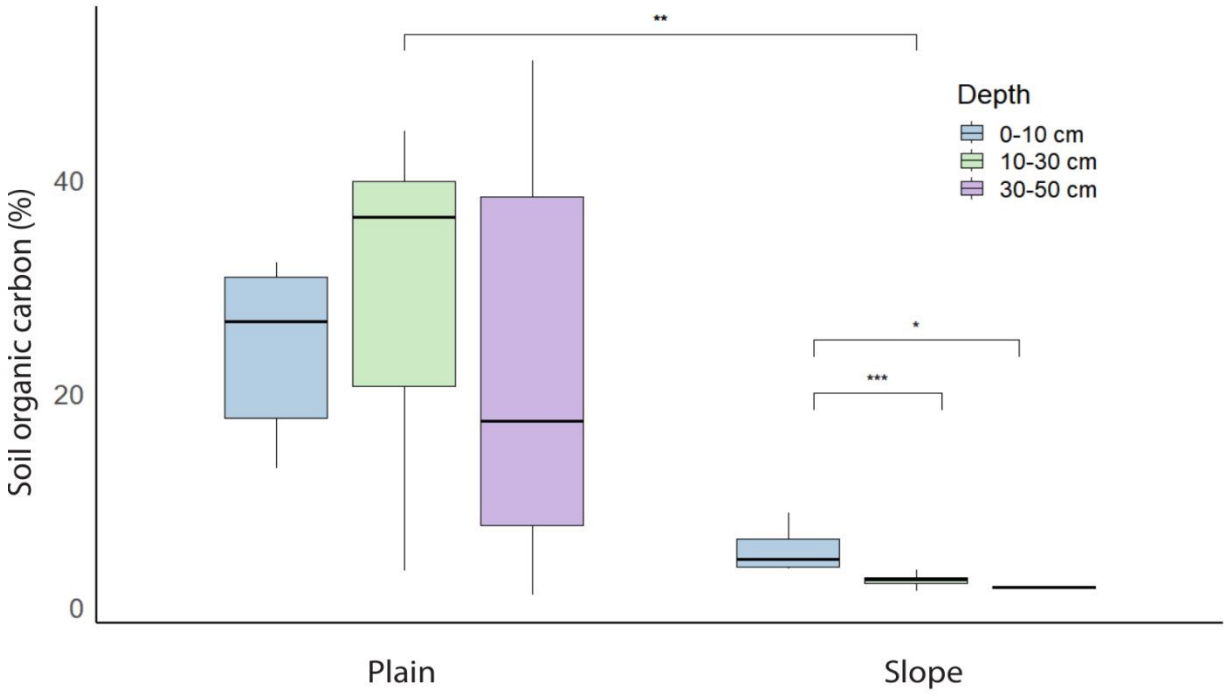

Figure 2: Soil organic carbon (SOC) content, expressed as percentage of dry soil mass, in plain and slope soils at three soil depths (0–10 cm, 10–30 cm, and 30–50 cm). Boxplots show the distribution of individual samples within each group; centre lines indicate medians, boxes indicate interquartile ranges, and whiskers indicate the range of the data excluding outliers. Asterisks indicate significant differences between plain and slope soils within each depth interval ($p < 0.05$, ** $p < 0.01$, *** $p < 0.001$). Sample numbers vary among depth intervals because the 30–50 cm layer was not available at all sampling locations (Table S1).*

View Article Online
DOI: 10.1039/D5EM01047K

Soil Organic Carbon Composition Differs by Landscape Position and Soil Depth

The composition of organic matter varied by landscape position and soil depth (Figure 3). Slope soils were enriched in polysaccharides (31.9 %), whereas plain soils contained higher proportions of phenols (20.9 %). The proportions of aromatics, lipids, nitrogen-containing compounds, and lignin was comparable between both types of soils. The relative contribution of aromatic compounds increased with soil depth from 23.3 % at 0 - 10 cm to 36.4 % at 30 - 50 cm, while the relative contriubtion of lignins decreased from 8.2 % at 0 - 10 cm to 2.1 % at 30 - 50 cm.

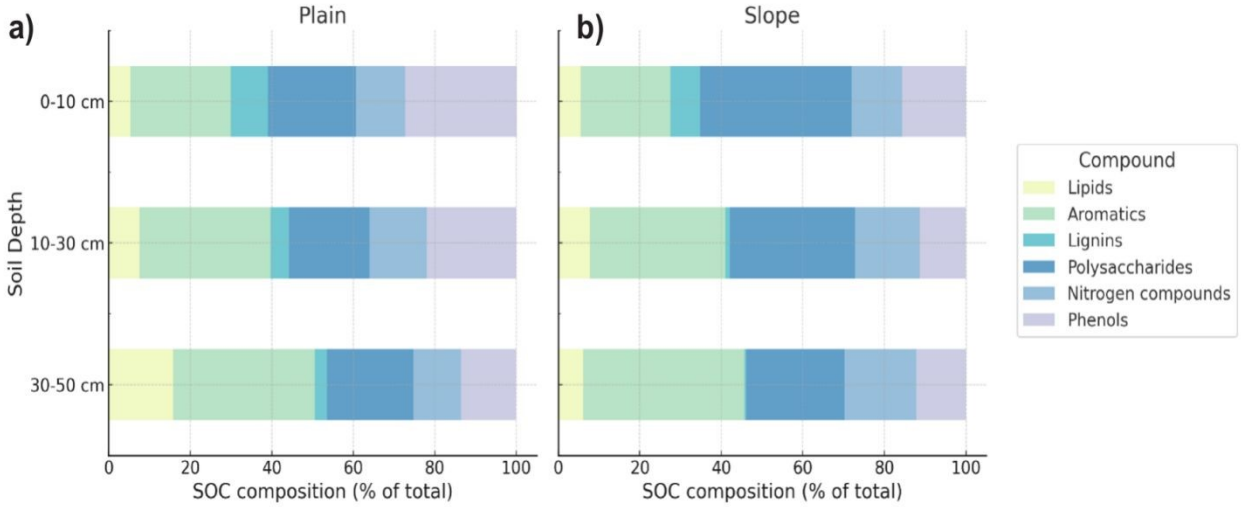

*Figure 3: Composition of soil organic carbon (SOC) in **a** plain and **b** slope soils, shown as the relative abundance (% of total identified SOC) of major compound classes determined by pyrolysis gas chromatography–mass spectrometry (Py-GC-MS). Compound classes include lipids, aromatics, lignins, polysaccharides, nitrogen-containing compounds, and phenols. Values represent individual soil samples across all sampled depths; relative abundances for each sample are provided in Table S3.*

Plain Soils Exhibit Soil Depth-Dependent Redox Zonation

Soil redox state was described the EAC and EDC values, which represent the contribution of the soils' pools of redox-active oxidised and reduced geochemical species, respectively. In plain soils, EAC and EDC values exhibited an inverse relationship, with EDC increasing from 0.12 ± 0.05 to 0.33 ± 0.07 mmol g^{-1} soil and EAC decreasing from 0.41 ± 0.10 to 0.16 ± 0.05 mmol g^{-1} soil from 0-10 cm to 30-50 cm soil depth, consistent with increasingly reducing conditions (Figure 4a). In contrast, slope soils showed low EDC values (e.g., 0.02 ± 0.01 at 10 cm) and constant EAC values (e.g., 0.48 ± 0.12 at 10 cm) across all soil depths, indicating oxic conditions (Figure 4b). We compared total electron exchanging capacity (sum of EAC and EDC) to elemental composition to attribute the EAC and EDC responses to geochemical phases (Figure S2). In plain soils, iron explained most of the redox reactivity, followed by sulfur. In slope soils, iron was the dominant redox-active phase, with a small contribution from redox-active organic matter.

View Article Online
DOI: 10.1039/D5EM01047K

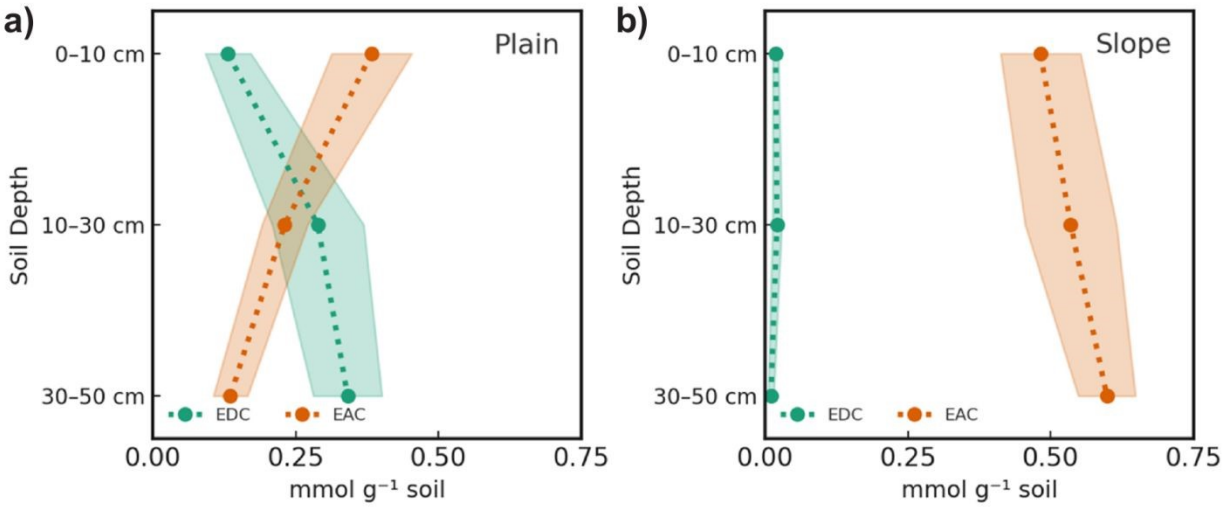

*Figure 4: Average electron donating capacity (EDC, green) and electron accepting capacity (EAC, orange) of **a** plain and **b** slope soils across the three sampled depth intervals. Capacities are expressed as mmol electrons per gram of dry soil and were determined by mediated electrochemical oxidation and reduction at pH 5.5 and +0.82 V and –0.51 V vs. SHE, respectively. Shaded areas represent the standard error of the mean.*

Microbial Community Composition and Functional Potential Are Linked to Soil Redox Conditions

Microbial community composition differed between plain and slope soils (Figure 5): plain soils had higher relative abundances of *Chloroflexota*, *Acidobacteriota*, and *Desulfobacterota*, whereas slope soils contained greater proportions of *Verrucomicrobiota*, *Thermoproteota*, and *Dormibacterota*. The heat map of functional genes (Figure 6) shows that plain soils exhibited higher relative abundances of genes assigned to nitrate, metal (Fe/Mn), and sulfate reduction across all soil depths, while slope soils had lower relative abundances of these genes. Canonical methanogenesis genes were not detected in the recovered MAGs, whereas genes attributed to methane oxidation (*Methylomirabilota*) were present in both landscape positions at low abundance.

Taxon–function links were identified between specific microbial lineages and key reductive processes (Table S3). *Chloroflexota* lineages (e.g., class *Anaerolineae*; class *Dehalococcoidia* lineages DSTF029 and SM23-31) correlated with nitrate-reduction genes. *Acidobacteriota* classes *Thermoanaerobaculia*, *Acidobacteriae*, and *Blastocatellia* correlated with Fe/Mn-reduction genes. Orders within *Desulfobacterota* (*Geobacterales*, BSN033, and *Desulfatiales*) correlated with sulfate-reduction genes.

View Article Online
DOI: 10.1039/D5EM01047K

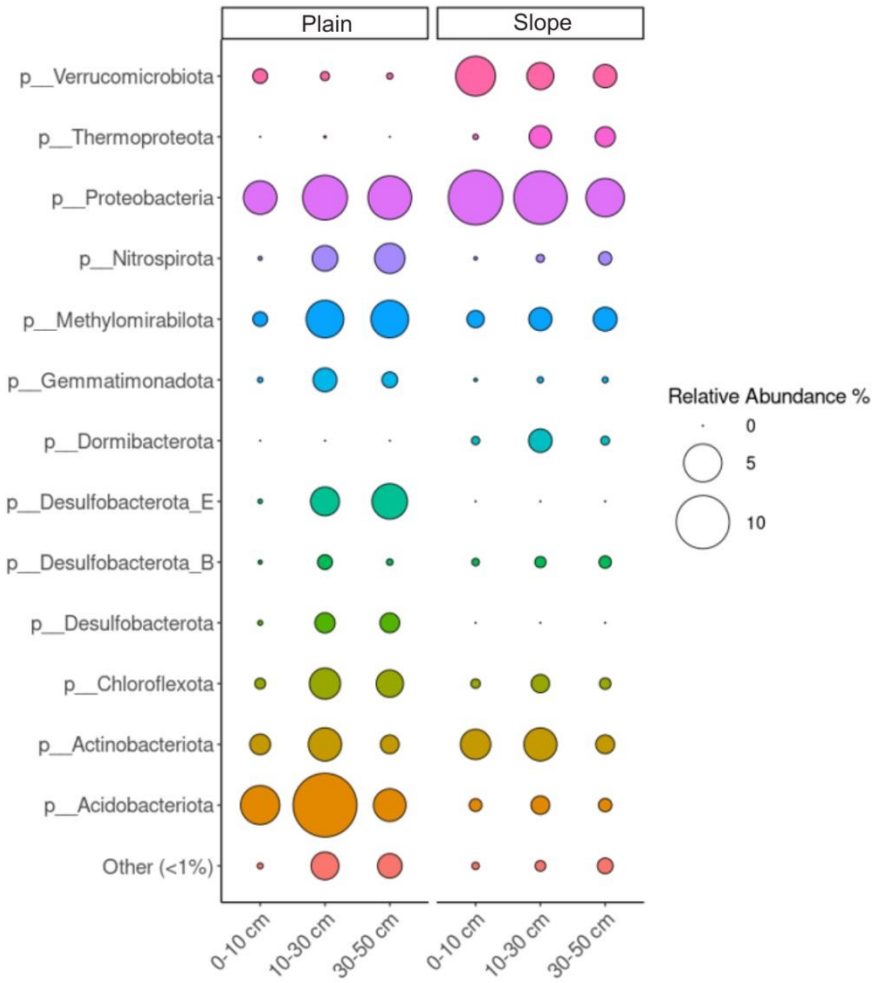

Figure 5: Microbial community composition in plain and slope soils across three soil depths. The plot shows the relative abundance of selected dominant prokaryotic phyla identified from metagenomic data. Circle size represents the relative abundance of each taxon within a given sample group, allowing comparison of taxonomic patterns across landscape positions and soil depths.

View Article Online
DOI: 10.1039/D5EM01047K

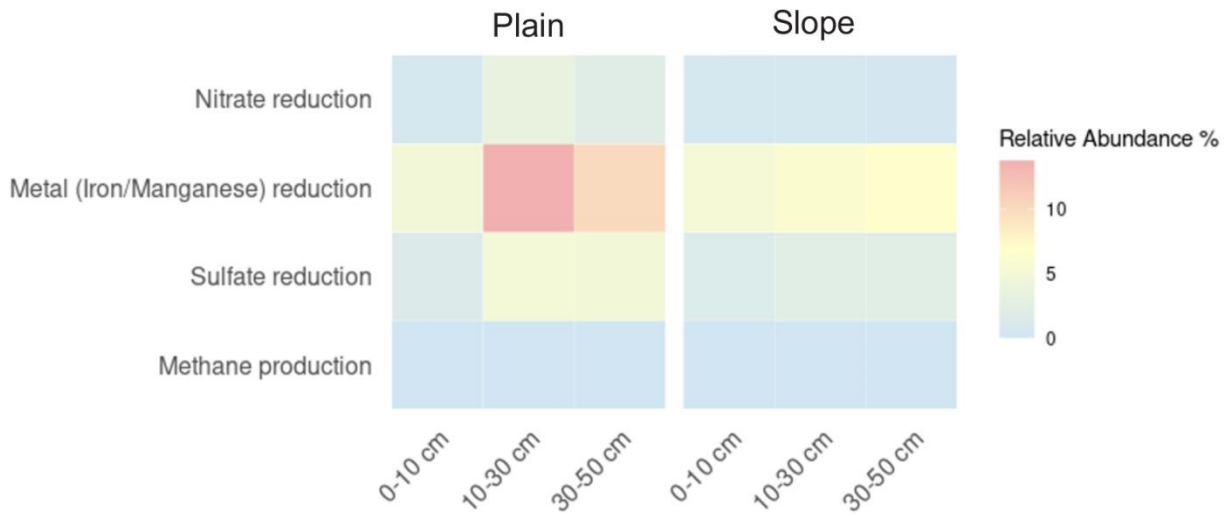

Figure 6: Heatmap of putative anaerobic microbial respiration pathways in plain and slope soils across three soil depths. Colours indicate the relative abundance of genes assigned to key metabolic pathways reconstructed from metagenomic data, including nitrate reduction, metal reduction, sulfate reduction, and methane production.

Microbiomes Exhibit Enhanced Metabolic Versatility and Greater Potential for Anaerobic Carbon Turnover in Plain Soils

We assessed the core set of metabolic functions relative to carbon turnover following the flowgram pipeline by [35]. Distribution of these functions, showing the proportion of metagenome-assembled genomes (MAGs) that encode the genes required for each transformation, indicate that SOC oxidation genes were present in 24.67 % of plain soil genomes (444 MAGs) versus 18.94 % in slope soil genomes (Figure 7). Fermentation potential was likewise greater in plain soil communities (12.85 %; 234 MAGs) than in slope soil communities (8.10 %). Hydrogen generation genes occurred in 11.61 % of plain soil genomes (231 MAGs) compared with 7.51 % of slope soil genomes, whereas hydrogen oxidation genes were found in 4.47 % and 1.30 % of genomes, respectively (74 MAGs). In contrast, acetate-oxidation genes showed slightly higher representation in slope soil communities (1.78 %; 28 MAGs) than in plain soil communities (1.30 %) while genes for ethanol oxidation and carbon fixation were detected at low levels in both settings (ethanol oxidation: 10.35 % plain, 9.55 % slope; carbon fixation: 1.09 % plain, 0.40 % slope). Methanotrophy genes were rare but detectable (0.66 % plain, 0.76 % slope; 21 MAGs), whereas canonical methanogenesis genes were not detected in the recovered assemblies. Overall, the higher prevalence of fermentation, hydrogen metabolism, and SOC-oxidation genes in plain soil MAGs indicates a larger genomic investment in anaerobic carbon turnover than in slope soils.

View Article Online
DOI: 10.1039/D5EM01047K

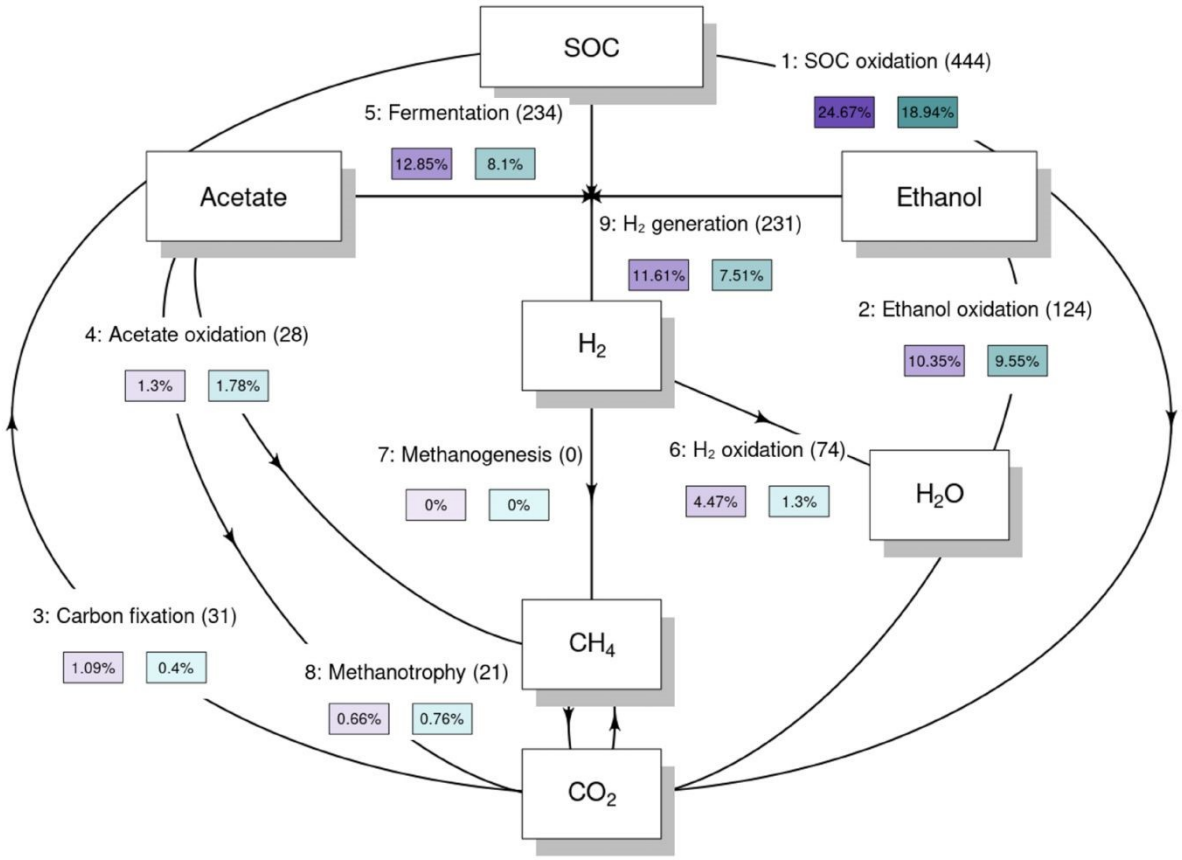

Figure 7: Soil organic carbon (SOC) transformations mediated by microbial communities in plain and slope soils. The flowgram illustrates SOC-related metabolic steps reconstructed from metagenomic data using a modified script from METABOLIC [35]. Each arrow represents a distinct transformation step, with boxes denoting key compounds involved. Arrow labels indicate the step number and transformation type, the number of genomes encoding the necessary genes (in brackets), and the relative abundance of those genomes in plain (purple) and slope soil communities (teal), expressed as a percentage of total community composition. Community-level genome abundance and function were inferred from metagenome-assembled genomes.

Microbial Community Composition Correlates with Soil Physicochemical Properties Across Landscape Positions and Catchments

Similarities of microbial community composition across catchments and landscape positions were assessed using an NMDS plot (Figure 8, supplementary environmental values in Table S1). Plain soil communities cluster on the bottom left, while slope soil communities cluster on the top right with minimal overlap between groups. Vectors for Ca content, soil pH, EAC, and phenols have the largest percentage value and point toward the plain soil cluster, indicating strong positive correlations with those communities. Conversely, vectors for polysaccharides, nitrogen-containing compounds, EDC, and clay content project toward the slope soil cluster. Sand and silt vectors plot between the two groups with intermediate vector lengths. Thus, variation in Ca content, pH, EAC, EDC, and specific SOC fractions (phenols,

View Article Online
DOI: 10.1039/D5EM01047K

nitrogen compounds, and polysaccharides) aligns with the primary ordination axis that separates plain and slope microbial assemblages.

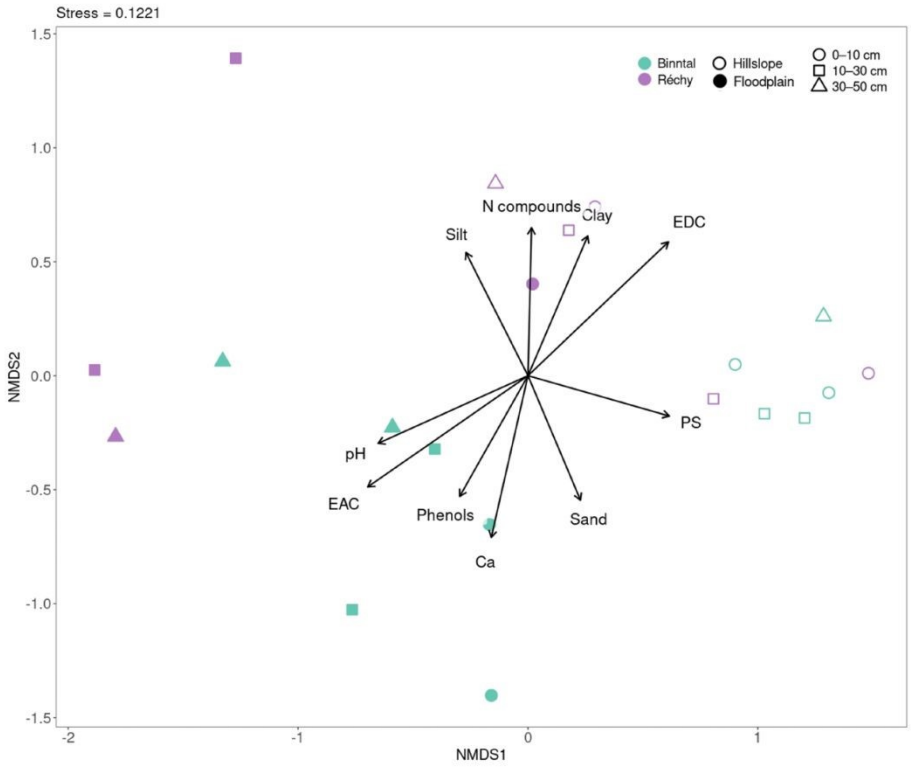

Figure 8: NMDS plot illustrating the microbial community composition of soils from two alpine headwater catchments, Binntal and Réchy, based on Bray-Curtis dissimilarity. Environmental vectors overlaid on the ordination indicate the direction and strength of correlations between environmental variables and microbial community composition. Vector length is scaled by the square root of the r^2 value, reflecting the strength of these correlations. The vectors represent the top ten environmental variables, selected based on descending r^2 values from envfit analysis. These variables include polysaccharides (PS), nitrogen compounds (N compounds), silt, clay, sand, soil pH, electron accepting capacity (EAC), calcium (Ca), phenols, and electron donating capacity (EDC). PERMANOVA attributes 23.3 % of the Bray–Curtis variation to landscape position ($R^2 = 0.2325$, $p = 0.001$) and 10.0 % to catchment identity ($R^2 = 0.0999$, $p = 0.030$); soil depth effects are negligible.

Discussion

Soil Redox State Is Linked to Soil Organic Carbon Quantity and Chemistry

Plain soils had substantially higher SOC content than slope soils, with nearly four times more carbon per g dry soil in the surface layer (0 - 10 cm; Figure 2). These differences mirrored

View Article Online
DOI: 10.1039/D5EM01047K

differences in soil redox state (Figure 4). In plain soils, conditions became increasingly reducing with soil depth. The observed EDC values likely reflect the accumulation of reduced organic compounds, ferrous iron, and sulfide, produced vial microbial respiration under past anoxic conditions. Iron was the major contributor to electron exchanging capacity and was therefore a key TEA in plain soils. In slope soils, no EDC was detected, suggesting that these soils were fully oxic. Most of the EAC response was explained by iron with some contribution from organic matter. The observed patterns in SOC content and soil redox state are therefore in agreement with our first hypothesis stating that soils on the plain exhibit anoxic conditions that are associated with higher SOC contents.

Differences in SOC composition between plain and slope soils are likely due to variations in organic matter inputs and preservation mechanisms. Plain soils were enriched in phenolic compounds, whereas slope soils contained higher proportions of polysaccharides (Figure 3). This pattern was linked to contrasting vegetation types and moisture regimes. On the plain, grasses and sedges produce litter rich in phenol-containing structural polymers, which are selectively preserved under periodically anoxic conditions because the degradation of phenolic compounds depends on extracellular oxidative enzymes, such as phenol oxidase and peroxidase [39,40]. In contrast, slope soils dominated by dwarf shrubs and upland herbs receive litter rich in easily degradable carbohydrates, which likely causes the higher abundance of polysaccharides. Across both landscape positions, we observed a decline in lignin-derived compounds and an increase in aromatic compound contributions with soil depth. The relative higher lignin content in surface soils likely reflects recent plant inputs from vascular tissue. Aromatic compounds are chemically more stable and persist under oxygen-limited conditions [39–41]. Combined, these findings indicate that as soil depth increases, lignin is progressively broken down or transformed, while less bioavailable aromatic structures accumulate.

The observed trends in SOC content and composition, and soil redox state align with the expected sequential microbial use of substrates based on reaction thermodynamics. Compared to polysaccharides, phenolic and aromatic compounds are chemically more reduced on average and therefore require higher energy input to be oxidized. Under anoxic conditions, this required energy input may outweigh the energy released upon redeuction of alternative TEAs, resulting in the accumulation of these compounds [4,7].

Microbial Community Composition and Potential Functions are Linked to Landscape Position and Soil Physicochemical Characteristics

Microbial community composition differed between plain and slope soils (Figure 5), with plain soils having higher relative abundances of potential microbial respiratory pathways, in agreement with our second hypothesis. These higher abundances may reflect seasonal moisture fluctuations and nutrient-rich conditions. Recurrent anoxic windows were associated with a rich assemblage of anaerobic microbial metabolisms, including the potential reduction of nitrate, iron, manganese, and sulfate, consistent with ongoing SOC turnover in the riparian corridor [10]. We found higher abundance of taxa commonly associated with anaerobic respiration at soil depth in plain soils, including members of the *Chloroflexota* or *Desulfobacterota* phyla [42], in line with the redox stratification inferred from EDC–EAC profiles. Conversely, slope soils were dominated by phyla such as

View Article Online
DOI: 10.1039/D5EM01047K

Verrucomicrobiota, *Thermoproteota* and *Dormibacterota*. These soils were well-drained and oxygen-rich and, in concert with lateral inputs of carbohydrate-rich litter, were associated with high-energy-yielding aerobic microbial respiration pathways. Canonical methanogenesis genes were not detected in the recovered MAGs from either plain or slope soils; however, non-detection in our metagenomic dataset does not necessarily indicate ecological absence. Methanogens may occur at low abundance, be restricted to deeper and more persistently waterlogged horizons, or remain in short and unbinned contigs that were not recovered during assembly and binning. The sequencing depth of shotgun metagenomics may also have been insufficient to recover rare methanogenesis genes, which can be difficult to detect in complex soil communities. By contrast, low-abundance methane oxidation genes were detected, suggesting that methane cycling may still occur in these soils even though methanogenesis potential was not recovered in the MAG dataset [15]. In addition, Group 3 and Group 1 NiFe hydrogenases were more highly represented in plain soils (Figure S3), consistent with greater redox flexibility and the capacity of these communities to alternate between fermentative and respiratory strategies as oxygen availability fluctuates [43].

Microbial community composition aligned with the observed differences in SOC composition across landscape positions (Figure 5). Microbial community assemblages in plain soils were associated with phenol-rich litter derived from hydrophilic grasses and sedges, which may require enzymatic capacities related to partial degradation under oxygen-limited conditions [43,44]. The association between phenolic compounds and anoxic conditions is consistent with slow decomposition of soil organic matter, and these compounds may also have contributed to the elevated EDC observed in plain soils by providing redox-active moieties that can function as extracellular electron shuttles [45,46]. In contrast, microbial communities in slope soils were dominated by fast-growing copiotrophs and were linked to polysaccharide-rich substrates, congruent with the higher proportion of depolymerisable carbohydrates we observed in these soils. Building on the previous discussion, the abundance of aromatic compounds increased with soil depth, whereas lignin-derived phenols decreased. Surface soil horizons were characterised by a higher relative abundance of lignin-derived compounds and by conditions consistent with microbial use of readily degradable polysaccharides and relatively rapid lignin turnover [47,48].

Several environmental variables influenced microbial community structure in plain and slope soils (Figure 8). EAC, Ca content, pH and phenolic content explained most variance in microbial community composition in plain soils. Calcium has previously been shown to stabilise SOC through cation bridging with negatively charged organic surfaces, potentially restricting microbial access to SOC [49]. Given the pH-dependence of these interactions and the propensity of alpine plain systems to experience seasonal water saturation [50], it is plausible that associated redox and pH fluctuations influenced microbial niche differentiation [51]. The observed association between phenolic content and microbial community composition may also be consistent with the presence of redox-active substrates linked to microbial groups capable of utilising these substrates either as carbon sources or as electron shuttles under oxygen-limited conditions. In slope soils, microbial assemblages were more closely aligned with polysaccharide content, EDC, and clay content. While mean EDC values were relatively low, the spatial variation across samples may point to micro-heterogeneity in the distribution of redox-active substrates, which could influence microbial

View Article Online
DOI: 10.1039/D5EM01047K

organisation even under well-drained conditions. Polysaccharides, derived from rapid cycling of plant litter, may provide readily accessible energy and were associated with copiotrophic lineages (notably several proteobacterial MAGs that our metagenomic analysis showed to be enriched in slope soils). Our results suggest that substrate quality, rather than the amount of SOC only, shape microbial assemblages under well-aerated conditions.

Our findings align with emerging evidence from other alpine regions, including the Qinghai–Tibet Plateau, where microbial community composition and carbon-cycling functions have been linked to gradients in soil moisture, pH, and wetland hydrology. Similar to our plain–slope contrast, studies from Tibetan alpine wetlands and riparian ecosystems suggest that water availability and associated geochemical conditions are key regulators of microbial functional structure [52]. Comparable process-level patterns have also been described in permafrost soils, where metagenomic analyses indicate that redox-sensitive pathways, especially iron cycling, can strongly influence microbial carbon turnover [53–55]. These similarities suggest that hydrology and redox state may represent general organising controls across cold-region soils, although the magnitude of their effects remains ecosystem-specific.

Our results also have implications for how alpine riparian carbon cycling may respond to future hydrological change. If climate warming lowers water tables in plain areas and increases soil oxygenation, the currently more reduced, phenol-rich SOC pool may become more susceptible to microbial decomposition as thermodynamic constraints on oxidation are relaxed. Conversely, if extreme precipitation events become more frequent on slopes, transient oxygen limitation may promote the temporary expansion of anaerobic microbial metabolisms and alter the balance between aerobic mineralisation and redox-sensitive carbon turnover. These process-based responses are consistent with the redox and substrate relationships observed in our study, although their magnitude will likely depend on local hydrology, vegetation, and mineralogical context.

Conclusions

Our work shows how microbial community composition varies across landscape positions from wet plain soils to drier slope soils in alpine riparian zones. Plain soils contained three to four times more SOC than adjacent slope soils, were enriched in phenolic compounds, had higher EDC values, and harbored microbial communities with genes for nitrate, iron, manganese, and sulfate reduction—features consistent with periodic anoxia and the accumulation of SOC due to thermodynamic limitations on microbial activity. In contrast, slope soils had lower SOC contents, were not reduced, had a higher proportion of labile polysaccharides, and microbial communities dominated by aerobic taxa. Together, these patterns demonstrate how moisture-driven redox regimes shape microbial potential and SOC composition, influencing the balance between SOC preservation and mineralization across the landscape. By comparing analogous landscape positions in two independent alpine catchments, our work provides a case study of how topographically driven redox gradients govern microbial ecology.

View Article Online
DOI: 10.1039/D5EM01047K

Several open questions remain regarding the role of microbial metabolism in carbon cycling in alpine riparian soils, particularly during seasonal transitions. Microbial communities may remain active beneath the winter snowpack, but their response to the spring melt pulse of dissolved organic carbon is not well understood. Future studies applying metatranscriptomics, extracellular enzyme assays, stable isotope probing, and targeted process measurements could help resolve these relationships more directly by linking microbial identity and activity to substrate use and carbon transformation under changing redox conditions. Such insights would clarify how seasonal and topographic variability regulates organic carbon turnover and ultimately the net carbon balance of alpine catchments.

Acknowledgements

The authors thank Lorenz Schwab, Antoine Wallart, and Eric Pizem for their support with soil sampling, Gordanna Pistoletti for technical assistance, and Massimo Bourquin for his help with publishing the metagenomics dataset. We also thank the Swiss National Science Foundation for financial support (Grant No. 212056).

Data Availability Statement

Soil physicochemical data in this article are available at https://doi.org/10.5281/zenodo.17710964. Metagenomic sequencing data generated in this study have been deposited in the European Nucleotide Archive https://www.ebi.ac.uk/ena/browser/view/PRJEB105115. All additional data supporting the findings of this study are provided in the article and its Electronic Supplementary Information.

References

1. Körner C. The alpine life zone. Springer International Publishing. 2021.

2. Davidson EA, Janssens IA. Temperature sensitivity of soil carbon decomposition and feedbacks to climate change. Nature 2006;440:165–173.

3. Duan X, Li Z, Li Y, Yuan H, Gao W, Chen X, et al. Iron–organic carbon associations stimulate carbon accumulation in paddy soils by decreasing soil organic carbon priming. Soil Biology and Biochemistry 2023;179:108972.

4. Gunina A, Kuzyakov Y. From energy to (soil organic) matter. Global Change Biology 2022;28:2169–2182.

View Article Online
DOI: 10.1039/D5EM01047K

5. Berhe AA, Kleber M. Erosion, deposition, and the persistence of soil organic matter: Mechanistic considerations and problems with terminology. Earth Surface Processes and Landforms 2013;

6. Pacific VJ, McGlynn BL, Riveros-Iregui D, Welsch DL. Landscape structure, groundwater dynamics, and soil water content influence soil respiration across riparian-hillslope transitions in the tenderfoot creek experimental forest, montana. Hydrological Processes 2011;25:811–827.

7. Boye K, Noël V, Tfaily MM, Bone SE, Williams KH, Bargar JR, et al. Thermodynamically controlled preservation of organic carbon in floodplains. Nature Geoscience 2017;10:415–419.

8. Schimel JP, Schaeffer SM. Microbial control over carbon cycling in soil. Frontiers in Microbiology 2012;3:348.

9. Zhang Z, Furman A. Soil redox dynamics under dynamic hydrologic regimes - a review. Science of The Total Environment 2021;763:143026.

10. Keiluweit M, Nico PS, Kleber M, Fendorf S. Are oxygen limitations under recognized regulators of organic carbon turnover in upland soils? Biogeochemistry 2016;127:157–171.

11. Philben M, Taş N, Chen H, Wullschleger SD, Kholodov A, Graham DE, et al. Influences of hillslope biogeochemistry on anaerobic soil organic matter decomposition in a tundra watershed. Journal of Geophysical Research: Biogeosciences 2020;125:e2019JG005512.

12. Philippot L, Chenu C, Kappler A, Rillig MC, Fierer N. The interplay between microbial communities and soil properties. Nature Reviews Microbiology 2023;1–14.

13. Romanowicz KJ, Crump BC, Kling GW. Genomic evidence that microbial carbon degradation is dominated by iron redox metabolism in thawing permafrost. ISME Communications 2023;3:1–11.

14. Waldrop MP, Chabot CL, Liebner S, Holm S, Snyder MW, Dillon M, et al. Permafrost microbial communities and functional genes are structured by latitudinal and soil geochemical gradients. The ISME Journal 2023;17:1224–1235.

15. Woodcroft BJ, Singleton CM, Boyd JA, Evans PN, Emerson JB, et al. Genome-centric view of carbon processing in thawing permafrost. Nature 2018;560:49–54.

16. Ruan Y, Ling N, Jiang S, Jing X, He J-S, Shen Q, et al. Warming and altered precipitation independently and interactively suppress alpine soil microbial growth in a decadal-long experiment. eLife 2024;12:RP89392.

17. Fu L, Xie R, Ma D, Zhang M, Liu L. Variations in soil microbial community structure and extracellular enzymatic activities along a forest–wetland ecotone in high-latitude permafrost regions. Ecology and Evolution 2023;13:e10205.

View Article Online
DOI: 10.1039/D5EM01047K

18. Dienes B, Mendoza O, Licini G, Bright K, Aeppli M. Interactive effects of landscape position and soil diversity drive the spatial variability of soil organic carbon concentration in subalpine soils of switzerland. EarthArXiv. 2026.

19. Richard J-L, Bressoud B, Buttler A, Duckert O, Gallandat J-D. Carte de la végétation de la région val de réchy-sasseneire (objet CPN 3.77, alpes valaisannes, suisse). Bulletin de la Murithienne 1993;111:9–40.

20. Frélechoux F, Gallandat J-D. Flore et végétation du haut val de binn entre chiestafel et le col de l'albrun. Bulletin de la Murithienne 1995;113:105–128.

21. Fick SE, Hijmans RJ. WorldClim 2: New 1-km spatial resolution climate surfaces for global land areas. International Journal of Climatology 2017;37:4302–4315.

22. Tolu J, Gerber L, Boily J-F, Bindler R. High-throughput characterization of sediment organic matter by pyrolysis–gas chromatography/mass spectrometry and multivariate curve resolution: A promising analytical tool in (paleo)limnology. Analytica Chimica Acta 2015;880:93–102.

23. Aeppli M, Voegelin A, Gorski CA, Hofstetter TB, Sander M. Mediated electrochemical reduction of iron (oxyhydr-)oxides under defined thermodynamic boundary conditions. Environmental Science & Technology 2018;52:560–570.

24. Aeppli M, Thompson A, Dewey C, Fendorf S. Redox properties of solid phase electron acceptors affect anaerobic microbial respiration under oxygen-limited conditions in floodplain soils. Environmental Science & Technology 2022;56:17462–17470.

25. Michaelis L, Hill ES. The viologen indicators. Journal of General Physiology 1933;16:859–873.

26. Thomas JH, Drake JM, Paddock JR, Conklin SD. Characterization of ABTS at a polymer-modified electrode. Electroanalysis 2004;16:547–555.

27. Andrews S. FastQC: A quality control tool for high throughput sequence data. 2010.

28. Chen S, Zhou Y, Chen Y, Gu J. Fastp: An ultra-fast all-in-one FASTQ preprocessor. Bioinformatics 2018;34:i884–i890.

29. Li D, Liu CM, Luo R, Sadakane K, Lam TW. MEGAHIT: An ultra-fast single-node solution for large and complex metagenomics assembly via succinct de bruijn graph. Bioinformatics 2015;31:1674–1676.

30. Gurevich A, Saveliev V, Vyahhi N, Tesler G. QUAST: Quality assessment tool for genome assemblies. Bioinformatics 2013;29:1072–1075.

31. Sahlin K. Strobealign: Flexible seed size enables ultra-fast and accurate read alignment. Genome Biology 2022;23:260.

View Article Online
DOI: 10.1039/D5EM01047K

32. Kang DD, Li F, Kirton E, Thomas A, Egan R, An H, et al. MetaBAT 2: An adaptive binning algorithm for robust and efficient genome reconstruction from metagenome assemblies. PeerJ 2019;7:e7359.

33. Chklovski A, Parks DH, Woodcroft BJ, Tyson GW. CheckM2: A rapid, scalable and accurate tool for assessing microbial genome quality using machine learning. Nature Methods 2023;20:1203–1212.

34. Chaumeil P-A, Mussig AJ, Hugenholtz P, Parks DH. GTDB-tk: A toolkit to classify genomes with the genome taxonomy database. Bioinformatics 2020;36:1925–1927.

35. Zhou Z, Tran PQ, Breister AM, Liu Y, Kieft K, Cowley ES, et al. METABOLIC: High-throughput profiling of microbial genomes for functional traits, biogeochemistry, and community-scale metabolic networks. Microbiome 2021;9:102.

36. Olm MR, Brown CT, Brooks B, Banfield JF. dRep: A tool for fast and accurate genomic comparisons that enables improved genome recovery from metagenomes through de-replication. The ISME Journal 2017;11:2864–2868.

37. Wood DE, Salzberg SL. CoverM: Read alignment statistics for metagenomics. Bioinformatics 2024;

38. Oksanen J, Blanchet FG, Friendly M, Kindt R, Legendre P, McGlinn D, et al. Vegan: Community ecology package. 2015.

39. Freeman C, Ostle N, Kang HS. An enzymic 'latch' on a global carbon store. Nature 2001;409:149.

40. Fenner N, Freeman C. Drought-induced carbon loss in peatlands. Nature Geoscience 2011;4:895–900.

41. Sinsabaugh RL. Phenol oxidase, peroxidase and organic matter dynamics of soil. Soil Biology and Biochemistry 2010;42:391–404.

42. Eilers KG, Debenport S, Anderson S, Fierer N. Digging deeper to find unique microbial communities: The strong effect of depth on the structure of bacterial and archaeal communities in soil. Soil Biology and Biochemistry 2012;50:58–65.

43. Piché-Choquette S, Constant P. Molecular hydrogen, a neglected key driver of soil biogeochemical processes. Applied and Environmental Microbiology 2019;85:e02418–18.

44. Yang Y et al. Deciphering factors driving soil microbial life-history strategies in restored grasslands. Environmental Microbiology Reports 2021;13:178–188.

45. Fenner N, Freeman C. Woody litter protects peat carbon stocks during drought. Nature Climate Change 2020;10:363–369.

46. Kappler A, Benz M, Schink B, Brune A. Electron shuttling via humic acids in microbial iron(III) reduction in a freshwater sediment. FEMS Microbiology Ecology 2004;47:85–92.

View Article Online
DOI: 10.1039/D5EM01047K

47. Dao TT, Mikutta R, Sauheitl L, Gentsch N, Shibistova O, Wild B, et al. Lignin preservation and microbial carbohydrate metabolism in permafrost soils. JGR Biogeosciences 2022;127:e2020JG006181.

48. Baldrian P. Microbial activity and the dynamics of ecosystem processes in forest soils. Current Opinion in Microbiology 2017;37:128–134.

49. Rowley MC, Grand S, Verrecchia ÉP. Calcium-mediated stabilisation of soil organic carbon. Biogeochemistry 2018;137:27–49.

50. Ma M, Zhu Y, Wei Y, Zhao N. Soil nutrient and vegetation diversity patterns of alpine wetlands on the qinghai-tibetan plateau. Sustainability 2021;13:6221.

51. Blagodatskaya E, Kuzyakov Y. Mechanisms of real and apparent priming effects and their dependence on soil microbial biomass and community structure: Critical review. Biology and Fertility of Soils 2008;45:115–131.

52. Wang X, Zhang Z, Yu Z, Shen G, Cheng H, Tao S. Composition and diversity of soil microbial communities in the alpine wetland and alpine forest ecosystems on the tibetan plateau. Science of the Total Environment 2020;747:141358.

53. Woodcroft BJ, Singleton CM, Boyd JA, Evans PN, Emerson JB, Zayed AAF, et al. Genome-centric view of carbon processing in thawing permafrost. Nature 2018;560:49–54.

54. Romanowicz KJ, Crump BC, Kling GW. Genomic evidence that microbial carbon degradation is dominated by iron redox metabolism in thawing permafrost. ISME Communications 2023;3:124.

55. Kang L, Song Y, Mackelprang R, Zhang D, Qin S, Chen L, et al. Metagenomic insights into microbial community structure and metabolism in alpine permafrost on the tibetan plateau. Nature Communications 2024;15:5920.

View Article Online
DOI: 10.1039/D5EM01047K

Data availability statement

Soil physicochemical data in this article are available on Zenodo at: https://doi.org/10.5281/zenodo.17710964

Metagenomic sequencing data generated in this study have been deposited in the European Nucleotide Archive at https://www.ebi.ac.uk/ena/browser/view/PRJEB105115

All additional data supporting the findings of this study are provided in the article and its Electronic Supplementary Information.